Evaluation of CO simulations and the analysis of the CO budget for Europe

G. Pfister,[1,2] G. Pétron,[1,3,4] L. K. Emmons,[1] J. C. Gille,[1] D. P. Edwards,[1] J.-F. Lamarque,[1] J.-L. Attie,[5] C. Granier,[4,6,7] and P. C. Novelli[8]

Received 25 February 2004; revised 2 July 2004; accepted 14 July 2004; published 6 October 2004.

[1] CO is a well-suited indicator for the transport of pollutants in the troposphere on a regional and global scale. For the study presented here, simulations of CO concentrations from a global chemistry transport model (MOZART-2), with the CO being tagged according to the emission type and the source region, have been used to diagnose the contributions of different processes and regions to the CO burden over Europe. Model simulations have been performed with both a priori emissions and an optimized set of CO surface emissions derived from the inversion of CO retrievals of the Measurements of Pollution in the Troposphere (MOPITT) remote sensing instrument. The annual mean difference between the modeled and the observed CO at 850 hPa over Europe is -38 ± 13 ppb with the a priori set of emissions and -7 ± 7 ppb when the optimized emissions are employed in the model. The general difficulties arising from an intercomparison of remote sensing data with model simulations are discussed. Besides data from MOPITT, ground-based CO measurements have been employed in the evaluation of the model and its emissions. The comparisons show that the model represents the background conditions as well as large-scale transport relatively well. The budget analysis reveals the predominant impact of the European emissions on CO concentrations near the surface, and a strong impact of sources from Asia and North America on the CO burden in the free troposphere over Europe. On average, the largest contribution (67%) to the anthropogenic (fossil and biofuel sources, biomass burning) CO at the surface originates from regional anthropogenic sources, but further significant impact is evident from North America (14%) and Asia (15%). With increasing altitude, anthropogenic CO from Asia and North America gains in importance, reaching maximum contributions of 32% for North American CO at 500 hPa and 50% for Asian CO at 200 hPa. The impact of European emissions weakens with increasing altitude (8% at 500 hPa). *INDEX TERMS:* 0368 Atmospheric Composition and Structure: Troposphere—constituent transport and chemistry; 0322 Atmospheric Composition and Structure: Constituent sources and sinks; 3360 Meteorology and Atmospheric Dynamics: Remote sensing; *KEYWORDS:* carbon monoxide, emissions, chemistry transport model, MOPITT, intercontinental transport

Citation: Pfister, G., G. Pétron, L. K. Emmons, J. C. Gille, D. P. Edwards, J.-F. Lamarque, J.-L. Attie, C. Granier, and P. C. Novelli (2004), Evaluation of CO simulations and the analysis of the CO budget for Europe, *J. Geophys. Res.*, *109*, D19304, doi:10.1029/2004JD004691.

1. Introduction

[2] The sources of atmospheric carbon monoxide (CO) are both anthropogenic and natural. Technological sources of CO are important in the Northern Hemisphere, and include transportation, combustion, industrial processes, and refuse incineration. Biomass burning dominates in the tropics and in the Southern Hemisphere, and includes burning of wood and agricultural waste, savanna burning, forest fires, and deforestation. Other CO sources are oxidation of methane and of nonmethane volatile organic compounds (NMVOCs), vegetation and soil, and oceans. There is a wide range in the different estimates of CO sources [e.g., *Graedel et al.*, 1993; *Bergamaschi et al.*, 2000; *Bey et al.*, 2001a; *Olivier et al.*, 2003] reflecting the uncertainty existing in our current knowledge of the CO budget.

[1]Atmospheric Chemistry Division, National Center for Atmospheric Research, Boulder, Colorado, USA.
[2]Institute for Geophysics, Astrophysics, and Meteorology, University of Graz, Graz, Austria.
[3]Advanced Study Program, National Center for Atmospheric Research, Boulder, Colorado, USA.
[4]Service d'Aéronomie, Université Paris 6, Paris, France.
[5]Laboratoire d'Aerologie, Observatoire Midi Pyrénées, Toulouse, France.
[6]CIRES/NOAA Aeronomy Laboratory, Boulder, Colorado, USA.
[7]Max-Planck-Institut für Meteorologie, Hamburg, Germany.
[8]NOAA Climate Monitoring and Diagnostics Laboratory, Boulder, Colorado, USA.

0148-0227/04/2004JD004691$09.00

[3] The CO concentrations in the troposphere hold interest from several perspectives. CO directly affects the concentration of the hydroxyl radical (OH), which is the primary oxidant of reduced species in the troposphere, and therefore influences the lifetime of many trace species. In much of the troposphere CO is responsible for about 60% of the OH removal [*Warneck*, 2000]. Furthermore, CO plays an important role as a precursor of tropospheric ozone production [e.g., *Levy et al.*, 1997]. Aside from its role in atmospheric chemistry, CO is an indicator for the transport of continental polluted air masses on a regional and global scale. The global average lifetime of CO is about two months, which means that CO remains in the troposphere long enough to be transported over large distances, but not long enough to be uniformly mixed. The actual CO distribution in the troposphere is therefore dependent on the magnitude, variability, and distribution of its sources and sinks, and on the transport over small and large scales.

[4] In the past, several investigations have been performed based on in situ measurements [e.g., *Seiler*, 1974; *Fraser et al.*, 1986; *Novelli et al.*, 1992] and model simulations [e.g., *Pinto et al.*, 1983; *Allen et al.*, 1996; *Brasseur et al.*, 1996] to study the global CO distribution and its dependence on sources, chemistry, and transport. Monitoring of CO over large scales is, due to the heterogeneous CO distribution, only practical with spaceborne remote sensing instruments. The first instrument to provide global CO measurements was the Measurement of Air Pollution from Satellite (MAPS) sensor [*Reichle et al.*, 1999], which was flown during four space shuttle missions. Global CO measurements taken continuously over a long time period were first taken by the Measurements Of Pollution In The Troposphere (MOPITT) instrument launched on board the NASA Terra satellite in December 1999 [*Drummond and Mand*, 1996]. In contrast to MAPS, which provided one piece of information, MOPITT data provide information about the vertical distribution of atmospheric CO concentrations.

[5] In this paper the vertically resolved CO concentrations retrieved from the MOPITT observations as well as ground-based in situ CO measurements are compared with simulations of the CO distribution from the global chemistry transport model MOZART-2 (Model for Ozone and Related Chemical Tracers). The purpose of this study is to analyze the budget of CO for Europe and the intercontinental transport of CO to Europe. We examine the contributions of transport, photochemistry, and surface emissions from various geographical regions to the CO concentrations over Europe.

[6] After a description of the MOPITT instrument and of the global chemistry transport model MOZART-2 in sections 2 and 3, respectively, we continue in section 4 with a comparison of CO measurements with model results. Section 5 presents an analysis of the modeled CO budget over Europe in terms of the contributions of sources, transport, and photochemistry. Finally, we summarize our findings and conclude in section 6.

2. Measurements of CO by MOPITT

[7] MOPITT is an eight-channel gas correlation radiometer designed to measure the vertical distribution of CO and the total column amounts of CO and CH_4 in the atmosphere with a nominal pixel resolution of 22 km by 22 km at nadir and a swath width of about 640 km. The orbital characteristics allow a global coverage in about three days. In this paper we make use of the vertically resolved CO mixing ratio, which is derived from radiance measurements in the 4.7 micron channels. CO concentrations are retrieved for clear sky conditions as well as for pixels covered by low clouds [*Warner et al.*, 2001]. For a more detailed description of the measurement technique and the retrieval we refer to *Deeter et al.* [2003].

[8] MOPITT data (data version V3) for the time period from the beginning of the measurements in March 2000 to May 2001 are currently available in validated status, and this data set has been used in the present study. The instrument experienced a failure in the cooler system in May 2001. Data for the phase after this failure are also available, and at the time of this work have been classified as "provisional status."

[9] Retrieval results from remote sensing instruments like MOPITT are fundamentally different from measurements with in situ instruments. For in situ measurements the vertical resolution is usually well approximated by a delta function, while for remote sensing observations the retrieved quantity is sensitive to some nonuniform weighting over altitude. The vertical sensitivity of the retrieved CO mixing ratio to the true profile is represented by the averaging kernels. Retrieving CO from the measured radiances is an ill conditioned problem. In the case of MOPITT the maximum likelihood retrieval algorithm is applied in the retrieval and this incorporates some amount of a priori information in the retrieved profile. The a priori CO profile and its covariance matrix used in the MOPITT retrieval are globally invariant and held constant with time. The a priori information was generated from a master set of 525 in situ profiles measured from aircraft during eight different field campaigns [*Deeter et al.*, 2003]. The averaging kernels as well as the a priori CO profile used in the retrieval need to be taken into account when interpreting the measured mixing ratios or comparing MOPITT data to in situ measurements or model simulations [*Rodgers*, 2000].

[10] The MOPITT retrievals include the CO mixing ratio for seven atmospheric levels (surface, 850 hPa, 700 hPa, 500 hPa, 350 hPa, 250 hPa, and 150 hPa), though these levels do not represent independent pieces of information [*Deeter et al.*, 2003]. For the three lowermost levels most of the information actually comes from the region between about 800 hPa and 500 hPa. This is evident in Figure 1 where we show the MOPITT averaging kernels for June and December 2000 for three retrieval levels: 850 hPa, 500 hPa, and 250 hPa. The data represent mean values over a region in central Europe of about 3° in latitude (45.7°N to 48.5°N) and 10° in longitude (9.7°E to 18.3°E) centered in Austria (this region is referred to hereinafter as "Austria"). Results for daytime as well as nighttime data are illustrated. As can be seen, the daytime averaging kernels for the lower levels are more sensitive to surface concentrations than the nighttime averaging kernels, with the difference being more pronounced in summer than in winter. While the 850 hPa averaging kernels for nighttime and daytime both peak at about 500 hPa in winter, the maximum sensitivity for daytime retrievals in summer months shifts to lower

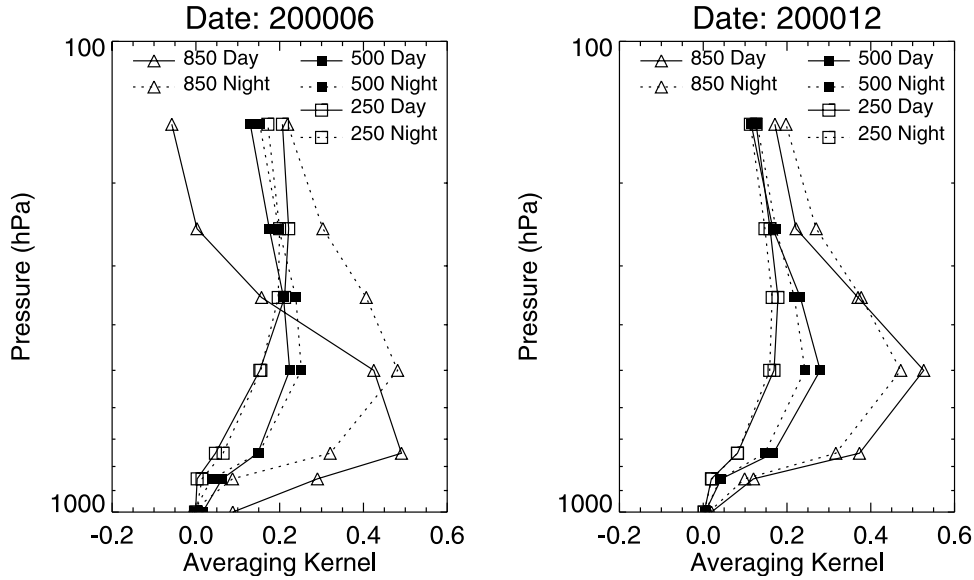

Figure 1. MOPITT averaging kernels (mean value over region Austria) for the 850, 500, and 250 hPa level. Daytime and nighttime values are shown for June and December 2000.

altitudes, about 700–800 hPa. For the higher levels the differences between day- and nighttime averaging kernels, and between summer and winter are less pronounced. The variations in the shape of the averaging kernels are caused by changes in the surface temperature and the thermal contrast between the surface temperature and the air temperature. A more detailed description of the averaging kernels and the information content of the MOPITT mixing ratios is given by *Deeter et al.* [2003] and is also available from the MOPITT home page at http://www.eos.ucar.edu/mopitt/.

[11] The uncertainties in the retrieved mixing ratios for individual MOPITT pixels as determined from the retrieval (including instrumental noise, calibration errors, radiative forward model errors, radiative transfer model input uncertainties, etc.) are generally highest for the lower altitude levels, and decrease with altitude. This is due to the low measurement sensitivity of MOPITT to the concentrations of CO near the surface, as is evident from the shape of the averaging kernels, and the associated larger contributions of a priori information. Uncertainties are also larger at high latitudes compared to tropical and mid latitudes. Over Europe, the estimated retrieval error for the CO mixing ratio is about 70 ppb or 40–60% for the surface level, and about 35–45 ppb or 20–30% at 850 hPa. For the 500 hPa level and above errors are typically below 20 ppb (below 20%). The MOPITT data validation [*Emmons et al.*, 2004] using aircraft in situ CO profiles indicates an average bias over all validation sites of 10 ± 18 ppb (11 ± 20%) for 850 hPa, and 4.4 ± 12 ppb (5 ± 12%) at 500 hPa. Differences for individual overpasses might reach values of up to about ±40 ppb (±50%).

3. Model Description

[12] MOZART-2 is a global chemistry transport model designed to simulate the global distribution of tropospheric ozone and its precursors. The model has been developed at the Atmospheric Chemistry Division at NCAR, the NOAA Geophysical Fluid Dynamics Laboratory, and the Max-Planck-Institute for Meteorology. MOZART-2 simulates the concentrations of 63 chemical species from the surface up to the lower stratosphere taking into account advection, convection, diffuse transport, surface emissions, photochemical conversion as well as dry and wet deposition. More information about the model is given by *Brasseur et al.* [1998] and *Horowitz et al.* [2003]. For the simulations used in the current study the model has been driven by meteorological inputs from the National Center for Environmental Prediction (NCEP) reanalysis in time steps of 6 hours. A horizontal resolution of 2.8° in latitude by 2.8° in longitude has been used with 28 sigma levels extending from the surface up to a pressure level of about 2 hPa. The model is run in time steps of 20 min, and model results are outputted as averages over 24 hours. Surface emissions of CO are employed as monthly averages.

[13] In contrast to the standard version of MOZART-2, the simulations used in the present study are based on an optimized data set for the CO surface emissions. This new set of emissions is the result of a prototype inversion scheme developed at NCAR/ACD in collaboration with the Service d'Aéronomie (CNRS/University of Paris). The inversion technique provides optimized estimates of CO surface emissions using MOZART-2 simulations and the MOPITT CO retrievals [*Pétron*, 2003].

[14] The inversion scheme developed to optimize the CO surface sources is a recursive and sequential Bayesian synthesis inversion. An a priori set of emissions has been built based on the EDGAR-v3 emissions inventory [*Olivier et al.*, 2003] extrapolated to the year 2000, on a new biomass burning emission inventory developed by C. Granier and J. F. Lamarque using fire counts from the Advanced Thermal Scanning Radiometer (ATSR) (personal communications), and on the GEIA (available at http://www.geiacenter.org) and *Müller* [1992] inventories for

Table 1. Annual Mean Optimized Emissions for the Different CO Types and Regions[a]

Region	Technological	Biofuel	Biomass	
Europe	70	11	14	
North Asia	6	3	15	
India	20	110	10	
China	101	112	22	
Southeast Asia	13	35	13	
Australia	3	<1	94	
North Africa (>15°N)	14	6	6	
North equatorial Africa (0°–15°N)	6	60	70	
South equatorial Africa	1	15	43	
South Africa	5	10	40	
Canada and Alaska	7	<1	2	
USA	122	8	11	
North Central America	8	3	30	
South Central America	3	1	31	
South America	9	3	42	
Type	30°N–90°N	0°–30°N	30°S–0°	90°S–30°S
Biogenic	96	69	89	4
Oceanic	2	3	3	3

[a]Emission values in Tg CO/year.

natural emissions. Uncertainties of 50% to 100% were assigned to each emission source.

[15] The observations used for the inversion are the MOPITT CO data at 700 hPa, binned on the model grid and averaged monthly for the time period April 2000 to March 2001. The relative total error attached to the observations is 100%, and all errors are expected to be uncorrelated. The impact of a monthly source is limited to 2 months. An inversion is performed for each month of observations and adjusts the emissions of the previous two months. The emissions of CO precursors are not optimized.

[16] The monthly emissions of three "anthropogenic" source types (technological activities, biofuel use, biomass burning) are optimized for 15 continental regions, and biogenic and oceanic emissions are optimized for four latitude bands (30°N–90°N, 0°–30°N, 30°S–0°, 90°S–30°S). The annual mean optimized emissions for the different CO types and regions are listed in Table 1. The natural emissions change only slightly when optimized, but the anthropogenic emissions are increased for most of the regions (on a global scale by 38%). Direct CO surface emissions for Europe, the USA, and Asia are enhanced by 23%, 37%, 50%, respectively. Further work has been done on the inversion algorithm, and the newest findings as well as a description of the regions and the inversion technique are given in a manuscript by G. Pétron et al. (Monthly CO sources inventory based on the 2000–2001 MOPITT satellite data, submitted to *Geophysical Research Letters*, 2004).

4. Comparison of Model Simulations With CO Measurements Over Europe

[17] In this section we evaluate the model simulations by comparing the optimized model CO distribution with observations. The first part (section 4.1) describes to what extent the MOZART CO fields agree with the CO profiles derived from the MOPITT data. From this comparison we gain an understanding of how well the model simulations represent the actual CO fields on a large scale over the course of a year. Because of the low sensitivity of the MOPITT measurements to surface concentrations and because MOPITT data have been used to improve the model emissions, we also evaluate the modeled CO distribution by comparing it with independent in situ surface observations described in section 4.2. The comparison with surface measurements allows us to investigate the validity of the surface emissions and of modeled CO surface concentrations. The continuous data series of the surface in situ data provides a look at the reproducibility of the seasonal changes by the model.

4.1. Comparison of MOZART and MOPITT CO Mixing Ratios

[18] The MOPITT retrieval provides a CO mixing profile with seven altitude levels from the surface up to 150 hPa. As already mentioned, the mixing ratio retrieved from the MOPITT observations is not directly representative of a single altitude, but is a weighted average over a broader altitude range. Therefore, when comparing MOPITT data with in situ measurements or model simulations it is necessary to take into account the vertical sensitivity of the MOPITT retrieval to the true CO profile. This is done by transforming the comparison profile (model or in situ) with the averaging kernels and the a priori CO profile for each of the MOPITT altitude levels [*Rodgers*, 2000; *Deeter et al.*, 2003]:

$$x_{\mathrm{rtv}} = x_a + A(x_{\mathrm{true}} - x_a). \quad (1)$$

The x_{rtv} in equation (1) stands for the retrieved or the transformed comparison profile, x_a is the a priori profile used in the MOPITT retrieval, x_{true} is the true or the comparison profile, and A is the averaging kernel matrix. In the following we will denote the modeled profile that has been processed with the a priori information and the averaging kernels as the "transformed" model profile.

[19] For the comparison of MOPITT and MOZART CO we applied the a priori information and the averaging kernels from each MOPITT pixel to the modeled CO profile of the nearest MOZART grid box. The transformed modeled and retrieved profiles have then been averaged over the model grid on a monthly basis. We carried out the intercomparison separately for day- and nighttime pixels, because of the diurnal differences inherent in the MOPITT averaging kernels. As mentioned earlier, MOPITT daytime retrievals typically have a higher sensitivity near to the surface due to the warmer surface temperatures. The separation into daytime and nighttime allows a more detailed analysis of the agreement between modeled and measured CO mixing ratios as a function of altitude.

[20] One constraint we applied in the comparison was to include only MOPITT pixels where the a priori fraction (an indicator for how much of the actual measurement contributed to the final retrieval) is less than 50% to avoid a distortion of the results by a too strong weighting toward the a priori information. The a priori is a necessary constraint in the maximum likelihood retrieval. The higher the a priori fraction, the more information in the retrieved MOPITT CO mixing ratio (the transformed model profile) comes from the a priori profile and the less from the measured radiances (the original model CO profile). This implies that the agreement between the retrieved and the transformed model mixing

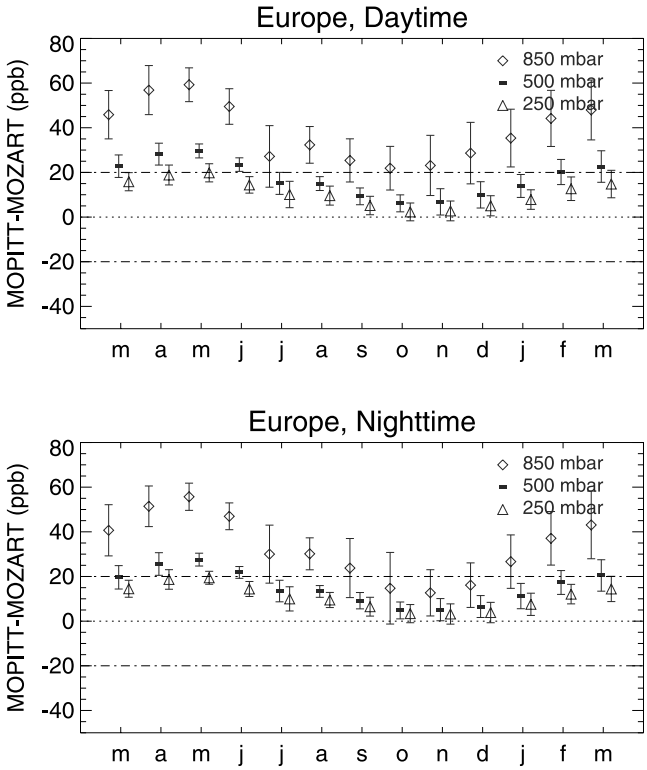

Figure 2. Monthly mean and standard deviation of the difference between the MOPITT and MOZART CO mixing ratio for three different pressure levels, shown for daytime and nighttime pixels separately. Average over the region Europe. A priori emissions have been used in MOZART.

ratios improves for a higher a priori fraction, because the true and the modeled profile are both weighted with the same averaging kernels and the same a priori information (equation (1)), and differences between them are reduced by the weighting.

[21] According to the MOPITT V3 Data Quality Statement, retrievals below 40 ppb at 500 hPa are probably erroneous, and for this reason these pixels were omitted. We consider the MOPITT layers from 850 hPa to 250 hPa in our study, but exclude the lowest (surface) and the highest (150 hPa). The reason is that the a priori fraction in the region of interest is usually larger than 50% for these two levels.

[22] The region considered in this study ranges from 35°N to 60°N, and 20°W to 40°E, and is hereinafter denoted as "Europe." The time period considered spans the months from March 2000 to March 2001. The comparison between observed and modeled CO mixing ratios averaged over the Europe region (spanning about 190 model grid boxes) for each month is summarized in Figures 2 and 3, with the results being shown separately for day and night. In Figure 2 the model results are based on the a priori emission inventory, while in Figure 3 the optimized emissions have been employed. The agreement between MOPITT and MOZART improves clearly when using the optimized emissions reducing the annual mean difference from -38 ± 13 ppb to -7 ± 7 ppb at 850 hPa, from -17 ± 8 ppb to 0 ± 4 ppb at 500 hPa and from -11 ± 6 ppb to 2 ± 3 ppb at 250 hPa. The correlation coefficients for the three altitude levels are calculated as 0.81, 0.70, and 0.65 when the a priori emissions are considered, and as 0.96, 0.92, and 0.92 when using the optimized emissions.

[23] In the following, we will have a closer look at the agreement between the modeled CO mixing ratios when employing the optimized emissions and the MOPITT retrievals (Figure 3). Monthly differences are in the range of about ±20 ppb (±20%) at 850 hPa for daytime, and differences are somewhat smaller for nighttime, about ±15 ppb (±15%). Largest discrepancies with regard to absolute and relative differences occur in springtime when the CO concentrations over Europe typically reach their maximum values. For the higher altitude layers the agreement for MOPITT and MOZART is better than ±10 ppb (±10%) for daytime and nighttime, i.e., the discrepancies are within the nominal MOPITT error bars. The standard deviation of the daily differences between the modeled and the measured CO mixing ratios is in the range of 10–15 ppb for the lower altitude layers, and about 5–10 ppb for pressure levels of 500 hPa and below. Again, somewhat smaller values for nighttime compared to daytime values are observed.

[24] Monthly averaged differences for individual model grid boxes might reach up to about 40 ppb at 850 hPa in cases when the observations are higher than the model values. Most of these extreme differences are observed for daytime pixels at the southern latitudes of the selected European region in spring and early summer. Even though the inversion procedure has already led to an increase in the surface emissions in the mid and high latitude regions of the Northern Hemisphere, this increase may not be strong enough to reproduce the amplitude in the CO spring peak

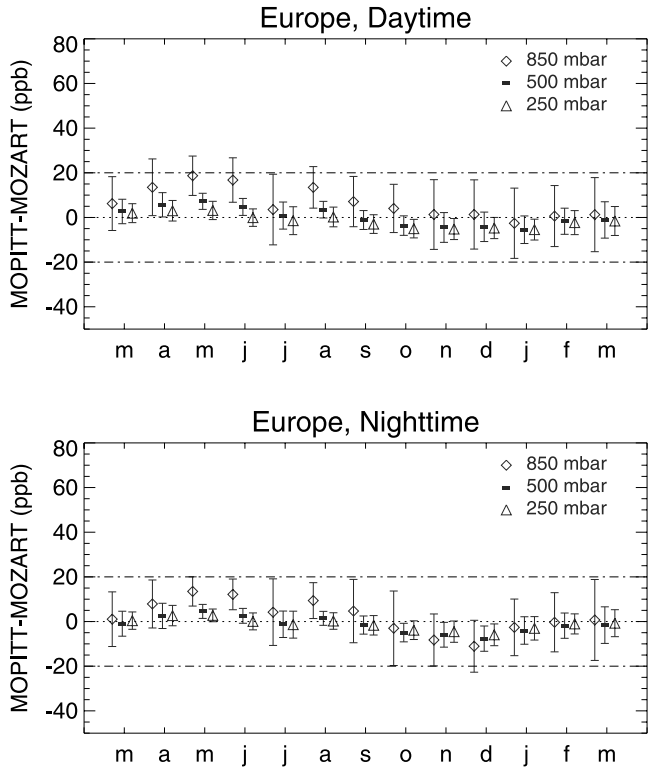

Figure 3. Same as Figure 2, except optimized emissions have been used in MOZART.

observed in the MOPITT retrievals. In situations when the modeled values are higher compared to the MOPITT retrieved CO mixing ratios the discrepancies are less pronounced, typically below 20 ppb. For higher altitude layers (500 hPa and altitudes above) the MOPITT and MOZART CO data over Europe differ by less than 10 ppb for individual grid cells.

[25] The results from the comparison show that the deviations between MOZART (optimized emissions) and MOPITT CO mixing ratios are of the order of the error bars derived from the MOPITT data validation (recall that the standard deviation of the differences over all validation sites has been determined as 18 ppb for 850 hPa and 12 ppb at 500 hPa), and also within the error bars derived from the MOPITT retrieval. The worse agreement at low altitude levels compared to higher altitudes can be explained by (1) uncertainties in the model surface emissions, (2) the different spatial resolution for MOZART and MOPITT, and (3) higher retrieval errors of the MOPITT data. Near the surface the CO concentrations are strongly influenced by local sources and the transport on small scale (boundary layer ventilation). Uncertainties in the geographical distribution of the emission sources in the model will mainly affect the lowermost levels whereas they have a lesser impact at higher altitudes. The closer to the surface, the more variable the observed CO concentrations are, in a spatial and temporal respect. This variability can be captured more strongly by the MOPITT data with a pixel resolution of about 22 km $\times$ 22 km than by the model having a grid cell size of 2.8° in longitude by 2.8° in latitude (roughly 200 km by 300 km for midlatitudes).

[26] The above mentioned factors can also help to explain the better agreement found for nighttime compared to daytime because the MOPITT retrievals for nighttime are typically less sensitive to the surface CO concentrations. In addition, the a priori fraction for nighttime pixels is somewhat larger compared to daytime pixels, i.e., nighttime pixels carry more a priori information than daytime pixels. At 850 hPa the a priori fraction for the selected daytime retrievals is typically in the range of about 20–30%, while it is around 40–50% for selected nighttime retrievals.

[27] To illustrate the vertical characteristics of the MOPITT-MOZART differences we show in Figure 4 four monthly averaged profiles and the corresponding standard deviations for the MOPITT daytime CO and the transformed MOZART CO profile for the region Austria (three model grid boxes). As additional information we have also included the original MOZART profile as well as the a priori profile used in the MOPITT retrieval. Modeled and measured profiles denote basically the same vertical dependence, in mean value and standard deviation, and agree within the above mentioned uncertainties. The standard deviation is typically smaller for the modeled profile.

[28] The data in Figure 4 demonstrate the change in the magnitude of the CO mixing ratio over Europe with season, but it must be kept in mind that seasonal changes in the MOPITT CO profiles are to some extent also influenced by accompanying changes in the averaging kernels. The comparison of the original MOZART profile with the transformed modeled profile gives an indication of the impact of the averaging kernels and of the a priori information on the "true" vertical CO distribution. This impact is clearly less than the seasonal change as seen in the MOPITT data, which is in the range of about 120 ppb to 180 ppb at 850 hPa, 90 ppb to 120 ppb at 500 hPa, and 90 ppb to 100 ppb at 250 hPa. Maximum CO concentrations are observed in springtime while minimum concentrations occur in autumn.

[29] The graphs, especially those for December and March, show also how important it is to limit the a priori fraction in the selection of the MOPITT retrieved CO data. The uncertainty in the retrieved CO mixing ratio is increasing with increasing value of the a priori fraction, and uncertainties might be large in cases when the a priori mixing ratio is far off from the actual profile (for example the CO profiles for winter and spring in Figure 4). The a priori fraction is less than 30% at all altitude levels for the data shown here, i.e., the impact of the a priori is rather small and information from the measured radiances strongly prevails. If we include pixels with a larger a priori fraction in our analysis the retrieved mixing ratio would spuriously be shifted toward lower values as the a priori information is clearly too low over Europe during the winter and spring months.

4.2. Comparison of MOZART With In Situ Measurements

[30] Ground-based in situ measurements of CO from various locations in Europe were used for an intercomparison with the modeled CO concentrations. We selected ground-based stations that are mainly characterized by background conditions and large-scale transport to account for the fact that the model gives an averaged picture of the situation on a large scale.

[31] In situ measurements from three ground-based background stations in Austria were provided by the Austrian Federal Environment Agency (UBA). Two of these sites, Vorhegg (46.68°N, 12.97°E) and St. Koloman (47.65°N, 13.23°E), are located in the mountains at an elevation of 1020 m asl (above sea level), the third, Illmitz (47.77°N, 16.77°E), is situated at 117 m asl. The stations are considered as background sites, but, to some extent, they are also influenced by nearby emission sources. This is true especially during wintertime when the anthropogenic surface emissions are largest. From the three sites, Illmitz experiences the strongest influence from local pollution sources, and Vorhegg is typically the least influenced (UBA Annual Report, 2000 and 2001; available in German language from http://www.ubavie.gv.at). The in situ measurements are available with a time resolution of 30 min, and a daily average has been calculated for the comparison with the model data. The accuracy for the CO in situ data is 10 ppb.

[32] For the comparison, the modeled MOZART CO concentrations were interpolated to the daily mean surface pressure measured at each site. Figure 5 shows the monthly mean values and the corresponding standard deviations for modeled and observed daily CO concentrations at the three stations from April 2000 to March 2001. As additional information we also show the results from a MOZART simulation using the a priori emissions. As can be seen the agreement of the model simulations at the three Austrian stations improved with the use of the "optimized" surface emissions compared to the model results referring to a priori surface emissions.

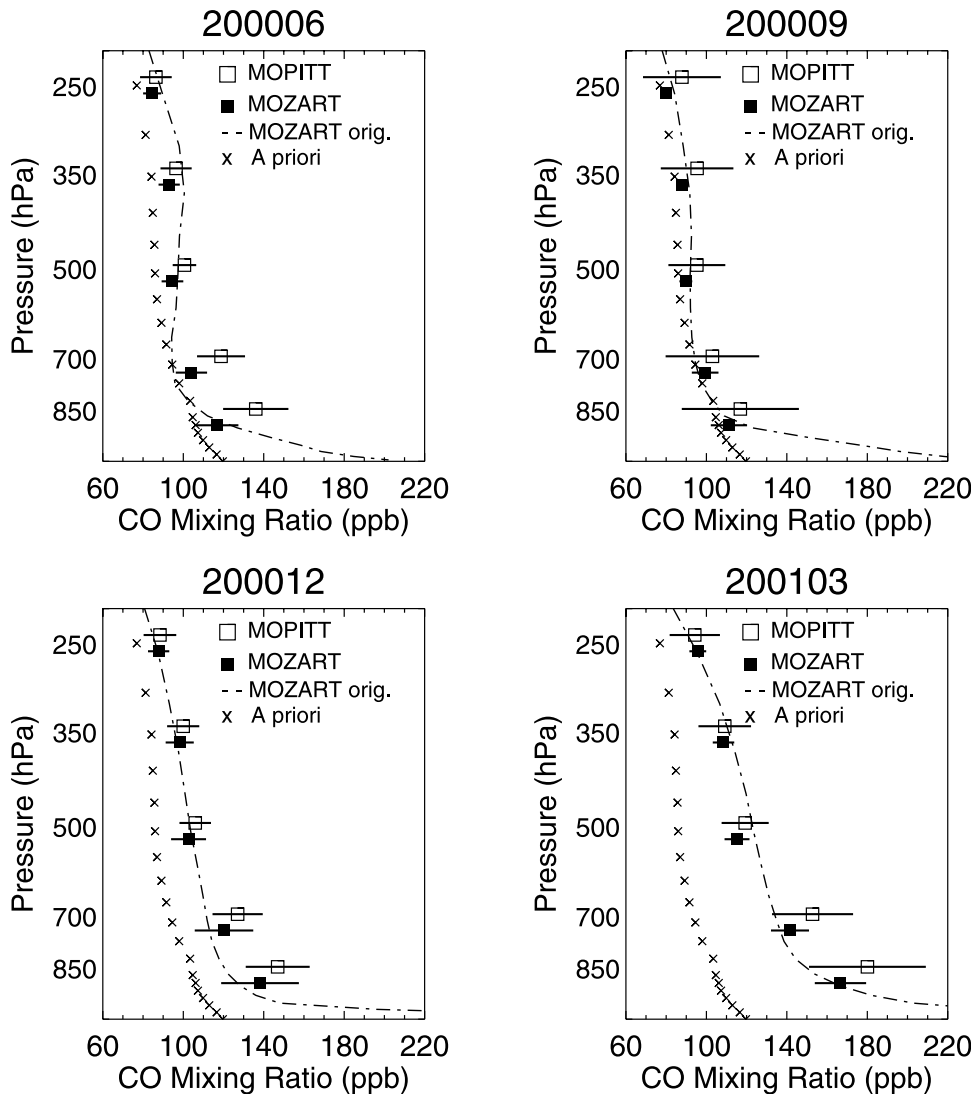

Figure 4. CO profiles averaged over the region Austria for June, September, December 2000, and March 2001. MOPITT and MOZART CO (transformed and original profile) are shown as well as the CO a priori profile included in the retrieval. Results are for daytime only. For clarity a small shift in altitude has been applied in plotting the data points.

[33] Differences between modeled and observed monthly mean CO and the associated variabilities are largest during the winter months, and are largest for Illmitz, which, for the most part, might be explained by the influence of local emissions and local transport condition. Largest differences for the mountain sites reach 40–50 ppb for Vorhegg during January to March, and around 40 ppb for St. Koloman in January and February. Both mountain sites actually fall into the same model grid box, but the observed monthly mean concentrations at these two stations might differ by up to about 30 ppb due to the impact of CO emissions of nearby sources and small-scale transport. Because of its spatial resolution, the model is unable to capture events happening on scales smaller than 200 to 300 km. On an annual mean the model (optimized emissions) underestimates the observations by 24 ± 14 ppb at Vorhegg, 21 ± 13 ppb at St. Koloman, and 20 ± 51 ppb at Illmitz. The model follows the seasonal variation fairly well at all three sites. The correlation between the monthly mean observed and simulated CO mixing ratios (with optimized emissions) is 0.95 for Vorhegg, 0.94 for St. Koloman, and 0.86 for Illmitz. The according mean differences of the model results based on a priori emissions with the observations are 49 ± 20 ppb at Vorhegg, 47 ± 17 ppb at St. Koloman, and 61 ± 58 ppb at Illmitz. The according correlation coefficients are 0.92, 0.95, and 0.86, respectively.

[34] The modeled CO concentrations have been, in addition, compared to surface in situ measurements taken at four stations of the Climate Monitoring and Diagnostics Laboratory (CMDL) network: Baltic Sea, Poland (“bal”, 55.5°N, 16.67°E, 7 m asl), Tenerife, Canary Islands (“izo,” 28.3°N, 16.48°W, 2360 m asl), Mace Head, Ireland (“mhd,” 53.33°N, 9.9°W, 25 m asl), and an ocean station in Norway (“stm”, 66°N, 2°E, 7 m asl). Tenerife and the Norwegian ocean station are located outside our region of interest, but reflect very well the situation at the northern and southern

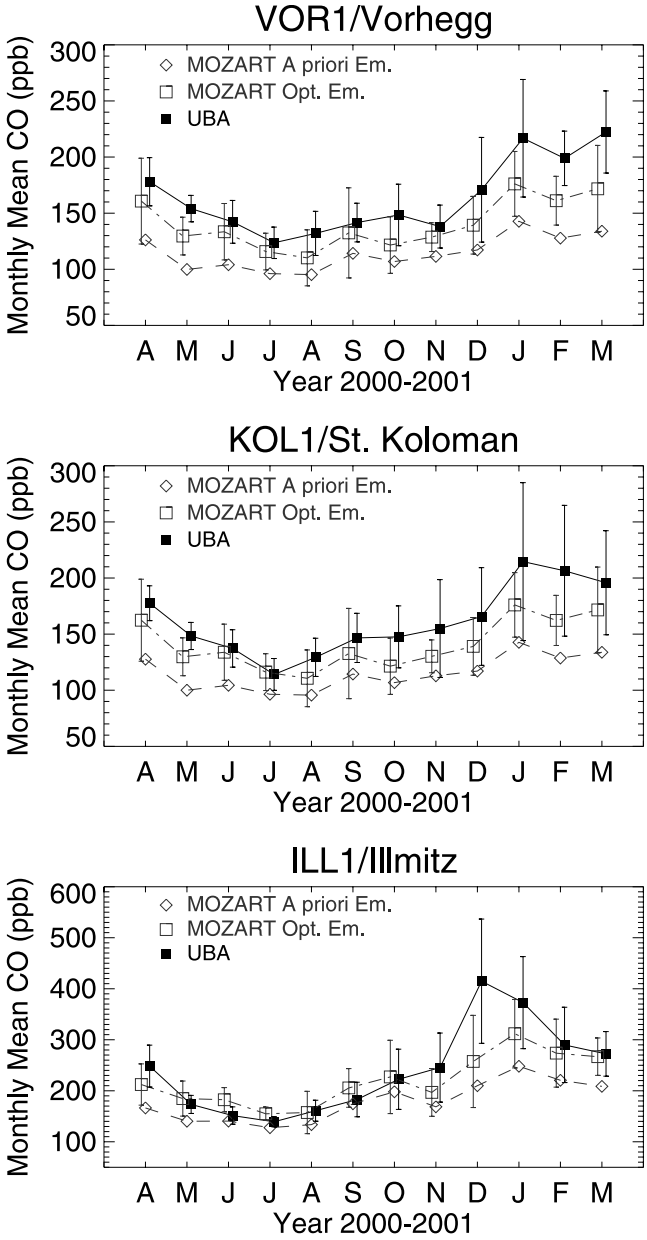

Figure 5. Comparison of MOZART CO concentrations with measurements at three Austrian sites Vorhegg (46.7°N, 13°E), St. Koloman (47.7°N, 13.2°E), and Illmitz (47.8°N, 16.8°E) from April 2000 to March 2001. MOZART simulations (based on a priori and optimized emissions) were interpolated to the surface pressure measured at the sites. Note the different scale for Illmitz. For clarity a shift of −0.1, 0, and 0.1 months has been applied in plotting the data.

boundaries, and therefore we include them in this intercomparison study. Information about the measurement sites and measurement technique is given by *Novelli et al.* [1994, 2003]. For calculating the monthly mean value of the modeled CO concentrations at each station only those days were used, for which observations were also available. The CMDL data were filtered according to the CMDL data selection process [*Novelli et al.*, 1992], but this filtering does not impact the comparison conclusions significantly.

[35] The monthly mean and the standard deviation of the measured and the modeled CO concentrations for each of the CMDL sites are shown in Figure 6 for the time period April 2000 to March 2001. Again, the model results for the a priori and the optimized emissions are shown. At Izana, Mace Head, and the ocean station the magnitude and also the seasonal variability of the observed CO mixing ratio is reproduced relatively well in the model. Largest absolute differences in the monthly mean values are observed for the Baltic Sea station. According to *Novelli et al.* [1998] Baltic Sea is a station representative of regionally polluted air since it is affected by industrialized north western Europe. This is also indicated by the higher CO mixing ratios at this station compared to the other sites. Model and observations differ the most during winter and spring when the variability in the monthly mixing ratios is high.

[36] CO concentrations at the ocean site are well reproduced by the model (optimized emissions) for the first months, but differences increase in autumn and winter 2000/2001 with the model concentrations being too high. This is in agreement with results from the MOPITT-MOZART comparison where the simulations for autumn and winter exceeded the measurements, especially at high latitudes. Best agreement is found for the site in Tenerife, which is due to its high altitude most of the time above the boundary layer and thus representative for background conditions. Good agreement is also shown for Mace Head. Mace Head too is considered as a typical background station, receiving mostly westerly winds from the North Atlantic [*Novelli et al.*, 1998]. At both sites we observe that the model simulations exceed the observations for most months, yet the differences are small.

[37] Mean annual differences between MOZART (optimized emissions) and the observations are -13 ± 12 ppb at Mace Head, and -4 ± 7 ppb at Tenerife. Larger biases are calculated for the other sites, -21 ± 14 for the ocean station, and -45 ± 41 ppb for Baltic Sea. Even though the absolute differences are large for Baltic Sea, the correlation is high (0.93). High correlation is also given for Tenerife (0.95), for Mace Head we derive a correlation of 0.94, and for the ocean station of 0.89. The according mean differences of the model results based on a priori emissions with the observations are 12 ± 12 ppb for Mace Head, 14 ± 7 ppb for Tenerife, 7 ± 18 for the ocean station, and -4 ± 30 ppb for Baltic Sea. The according correlation coefficients are 0.90, 0.90, 0.80, and 0.91.

[38] By analyzing the improvement achieved from using the optimized emissions for the surface sites it has to be kept in mind that the optimization of the surface emissions is applied to an entire region, e.g., the entire emissions of Europe are scaled by a single factor. It is important to understand that any errors in the geographical distribution within a selected region existing in the a priori emissions will translate into the optimized emissions. The comparisons described in here reflect this issue. While the agreement of the modeled CO field averaged over Europe with MOPITT retrievals clearly improves, it may not be the case for all locations within Europe.

[39] In summary, the comparison of MOZART with the in situ data reflects the large variability in the CO concentrations that exist on small temporal and spatial scales, and that the model typically does not capture these features.

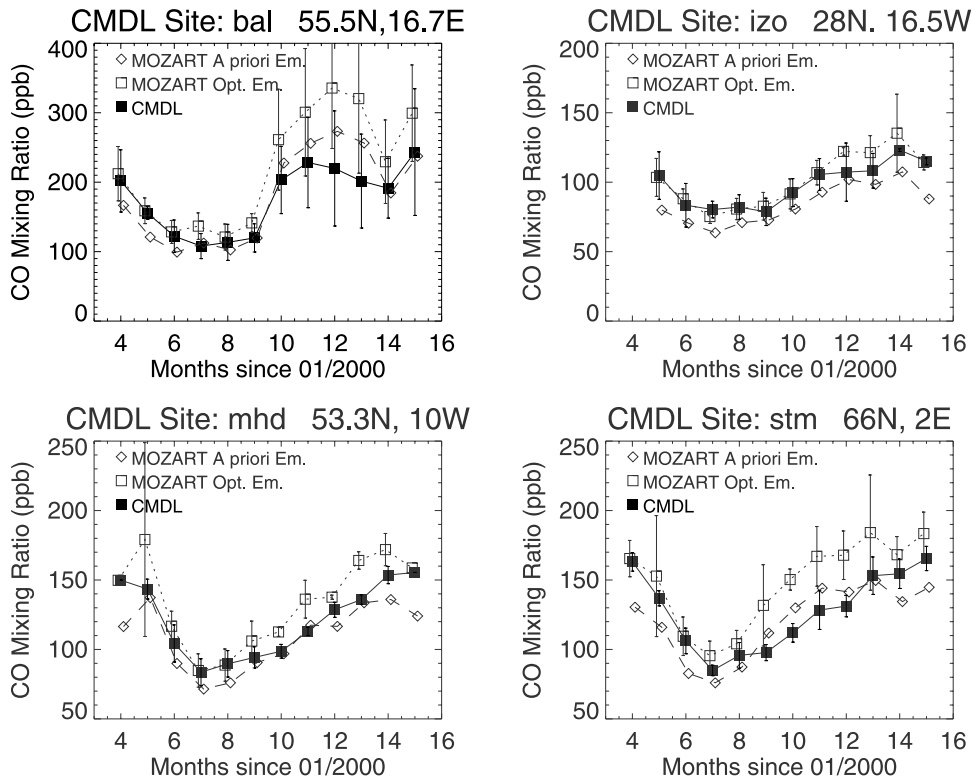

Figure 6. Comparison of MOZART CO concentrations with measurements at four CMDL sites from April 2000 to March 2001. MOZART simulations (based on a priori and optimized emissions) for the lowermost layer are used. Note the different scales. For clarity a shift of −0.1, 0, and 0.1 months has been applied in plotting the data.

However, when longer time periods (e.g., a month) and larger regions (e.g., Europe) are considered, the model simulations seem to fairly well represent the actual situation. On average, the differences are less than about 25 ppb near the surface, and less than about 15 ppb in the free troposphere. The high correlation between monthly mean observed and modeled CO as determined from MOPITT and surface in situ data demonstrates a good representation of seasonal variations in the model.

5. Analysis of the Modeled CO Field

[40] The comparison of the simulated CO fields from MOZART with remote sensing and in situ data over Europe showed that the model is capable of representing the actual situation on the large scale relatively well, and that it also captures seasonal variations. On a large scale the agreement between the modeled CO fields and observations improved with the use of optimized emissions. For this reason, the following analyses are based on model simulations employing the optimized CO emissions inventory.

5.1. CO Field Over Europe

[41] To get an overview of the CO budget characteristics over Europe we begin with a description of its spatial and seasonal changes. In Figure 7 the modeled annual mean CO distribution over Europe (averaged over the time period April 2000 to March 2001; model grid resolution of 2.8° by 2.8°) is shown for four different altitude levels. Near the surface, the CO mixing ratio is mainly driven by regional surface emissions, and largest annual mean concentrations (∼300–350 ppb for the model spatial resolution) are observed over regions where emissions are strongest, i.e., central Europe and parts of eastern Europe. Lowest CO mixing ratios in the range of about 140 ppb are evident over the coastal areas of western Europe.

[42] With increasing altitude the annual mean distribution becomes less influenced by regional emissions and small-scale transport within the boundary layer, but photochemistry and the distribution by large-scale wind systems (west wind zone) gain in importance. As a result, the CO distribution becomes, on average, more strongly latitude dependent with CO mixing ratios increasing from south to north in the lower free troposphere. At 800 hPa the CO mixing ratio over the selected region is in the range of about 105–135 ppb, and at 500 hPa the modeled CO concentrations cover the range ∼95–115 ppb. Very little spatial variability in the annual CO mixing ratio is evident at 200 hPa, the concentrations show values around 80 ppb and vary only by a few ppb.

[43] In the course of a year the CO concentrations over Europe experience quite large variations as illustrated by the CO observed at the surface stations. The seasonal changes of atmospheric CO concentrations are primarily influenced by the seasonality of photochemical loss and production, and therefore by the annual change in solar insolation, but also by seasonal variations in the surface emissions, changes in circulation patterns, and by convection. Averaged over Europe, the seasonal amplitude (no graph shown) might be as large as about ±50–60 ppb near the surface, about

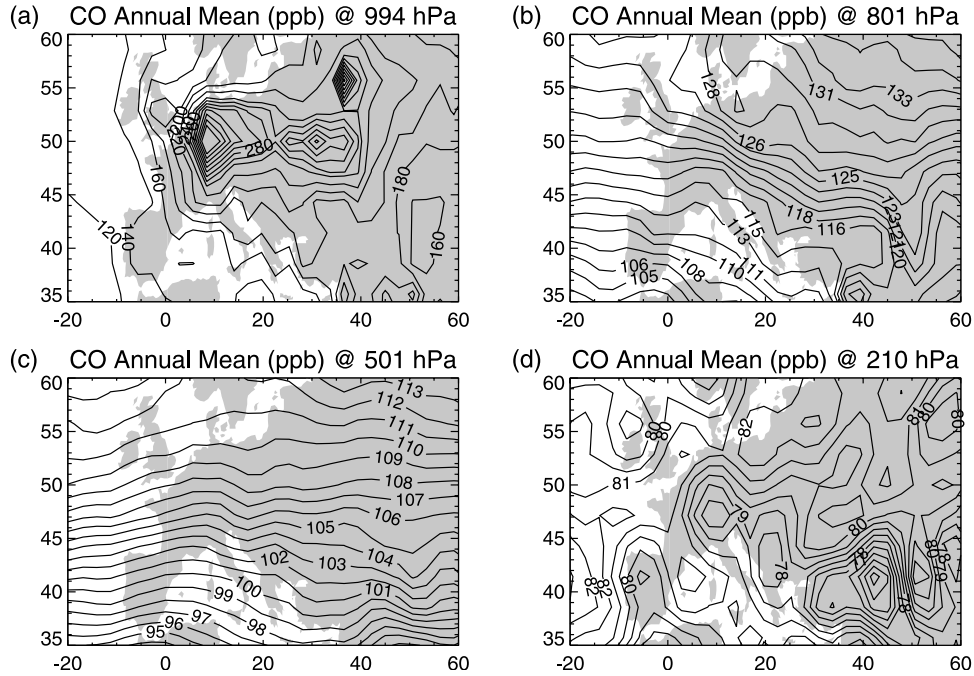

Figure 7. Annual (April 2000–March 2001) mean CO concentration over Europe for four different altitude layers: (a) surface layer (994 hPa), (b) 801 hPa, (c) 501 hPa, and (d) 210 hPa.

±30 ppb at 800 hPa, and about ±20 ppb at 500 hPa (recall this is comparable to the seasonal amplitude observed in the MOPITT data). Largest concentrations are seen around wintertime and early spring, when the lifetime of CO is longest and the emissions are strong. Lowest values are evident in summer, i.e., when the atmospheric OH concentrations are higher due to intense solar insolation resulting in faster oxidation of CO molecules and a reduced CO lifetime. With increasing altitude (1) the amplitude of the seasonal variations is declining, and (2) the maximum shifts toward summer. At 100 hPa the maximum is observed in summer, and the minimum in winter. The amplitude of the seasonal variation, though, is only a few ppb at this altitude.

5.2. CO Budget Over Europe

5.2.1. Tagged Model Emissions and the Off-Line Chemistry Model

[44] Global atmospheric chemistry transport models [e.g., *Bey et al.*, 2001b; *Wild and Akimoto*, 2001; *Li et al.*, 2002] as well as, for example, Lagrangian particle dispersion models [*Stohl et al.*, 2002, 2003] or trajectory models [*Stohl and Trickl*, 1999; *Forster et al.*, 2001] are well suited to investigate the intercontinental transport of pollutants. A very practical way to track the origin of CO in the MOZART model is to tag CO molecules according to the type and location of their direct surface sources and this way follow their transport path and chemical decay. Analyses based on tagged emissions have been performed for CO by *Granier et al.* [2000] and *Lamarque and Hess* [2003]. We used "tagged model simulations" in our study to track down sources that strongly contribute to the CO concentrations over Europe.

[45] The off-line chemistry model employed for the tagged model run uses OH fields that have been saved every six hours in a model run with online chemistry (the model run where total CO concentrations are determined). Combining the tagged CO concentrations with the CO concentrations from the full model run gives information about the contribution of CO produced by photochemical processes.

[46] The tagged model runs performed for the current study handle 53 different types of CO emissions as described in section 3. No tagging has been applied with regard to the time of the emissions. The strongest anthropogenic sources are found predominately in the Northern Hemisphere and are assigned for the regions China (234 TgCO/yr), USA (mainland USA excluding Alaska; 140 TgCO/yr), India (140 TgCO/yr), north equatorial Africa (135 TgCO/yr), Australia (97 TgCO/yr), Europe (95 TgCO/yr), and Southeast Asia (60 TgCO/yr). These regions amount for 75% of all anthropogenic emissions. Biogenic emission sources (global total of 257 TgCO/yr) are about one fourth of the strength of all anthropogenic emissions, and are about a factor of 2 stronger in the Northern Hemisphere compared to the Southern Hemisphere. Oceanic emissions (global total of 10 TgCO/yr) contribute to a much smaller extent to the CO global source and are less than 1% in strength of the total CO source.

5.2.2. Origin of CO Over Europe

[47] In the following we will use simulations from the tagged model run to study the origin of CO over Europe. In Figure 8 we show the contributions of various sources to the CO burden over Europe for two altitudes (surface and 500 hPa). The relative share of the photochemically produced CO on the total CO over Europe is largest at high altitudes, and largest in summertime with the amplitude of the seasonal variability decreasing with altitude. Averaged over the Europe region, the photochemically produced CO accounts for about 15% of the total CO concentrations close to the surface in winter, and for about 40% in summer.

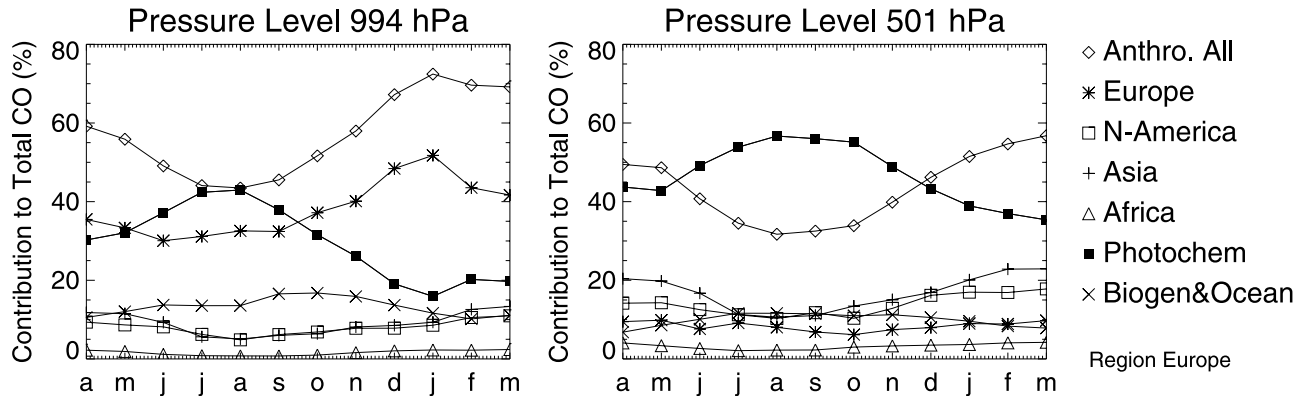

Figure 8. Contribution (%) of anthropogenic emissions from various sources as well as photochemical and biogenic and oceanic CO on the total CO concentrations for the region Europe, April 2000 to March 2001. (left) Surface layer (994 hPa); (right) 501 hPa.

The contribution increases with altitude and reaches about 35–55% at 500 hPa; at 200 hPa (not shown) more than about half of the CO is produced photochemically. Near the surface, the fraction of photochemical CO to the total CO mixing ratios is typically smallest near strong anthropogenic sources and the latitudinal dependence relatively weak. In the free troposphere, the contribution of photochemical CO is more strongly stamped by latitudinal variations with largest values at low latitudes. Near the surface, about 10–15% of the total CO concentrations originate from biogenic emissions, and the maximum impact occurs in autumn. This contribution decreases with altitude as expected for a surface source, and it reaches values in the range of about 5% and less at 200 hPa.

[48] The contribution of anthropogenic CO to the total CO mixing ratios, averaged over Europe, is in the range of about 40–70% close to the surface, ~30–60% at 500 hPa, and 30–40% at 200 hPa (not shown). Strongest impact is evident at the end of winter and in spring, and smallest impact occurs during summertime. In Figure 9 we show the annual mean contributions of CO emitted in various source regions to the anthropogenic and total CO concentrations over Europe. The contribution of anthropogenic emissions on the CO load over Europe mainly originates from sources in Europe, North America, Asia, and to some extent North Africa. Intrusions from other regions are negligible.

[49] The total anthropogenic CO concentrations over Europe as a function of month and altitude are shown in Figure 10a giving an insight into the magnitude of the anthropogenic activities impact on this region. Near the surface, the strongest contribution to the anthropogenic CO fields is attributed to regional (i.e., European) sources, but with increasing altitude in the atmosphere, the impact of European sources weakens as CO is spread and transported horizontally. On a spatial and annual average, the contribution decreases from about 67% at the surface to ~10% at 200 hPa. The decreasing impact with increasing altitude is also seen in Figure 10b where the contribution of European CO on the total anthropogenic CO load over Europe is depicted as a function of month and altitude. In the free troposphere, the largest contribution of European sources to the anthropogenic CO over Europe is typically seen in the summer months, which might be due to increased convection, and the decreased lifetime of CO during this season.

[50] Together with the decreasing impact of European sources on the anthropogenic CO at higher altitude, intrusions from other continents become more pronounced as seen in Figure 9 as well as Figures 10c and 10d showing the contributions for Asian and North American sources, respectively. On an annual and spatial average, CO from North American sources shows the maximum influence on the anthropogenic CO levels over Europe, ~35%, at altitudes around 500 hPa, while the main impact from Asian sources is evident at the highest altitude levels with maximum values of about 50%.

[51] For the North American contribution it is mainly sources in the USA region that affect the CO field over Europe, and impact from the Canada and Alaska region is typically only a few percent at all altitudes. On average, the anthropogenic sources in the USA amount to about 13% of the anthropogenic CO load over Europe at the surface, and the impact reaches a maximum at around 500 hPa with contributions being in the range of 30%. At 200 hPa the impact is 21%.

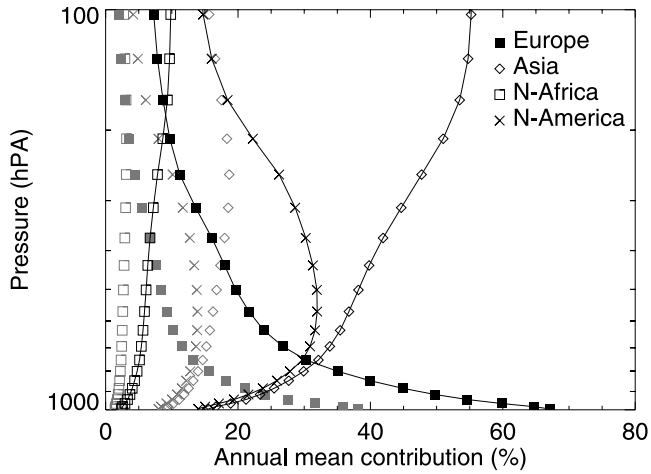

Figure 9. Annual mean contribution (%) to the anthropogenic (black) and total (gray) CO concentrations over Europe for some source regions as function of altitude.

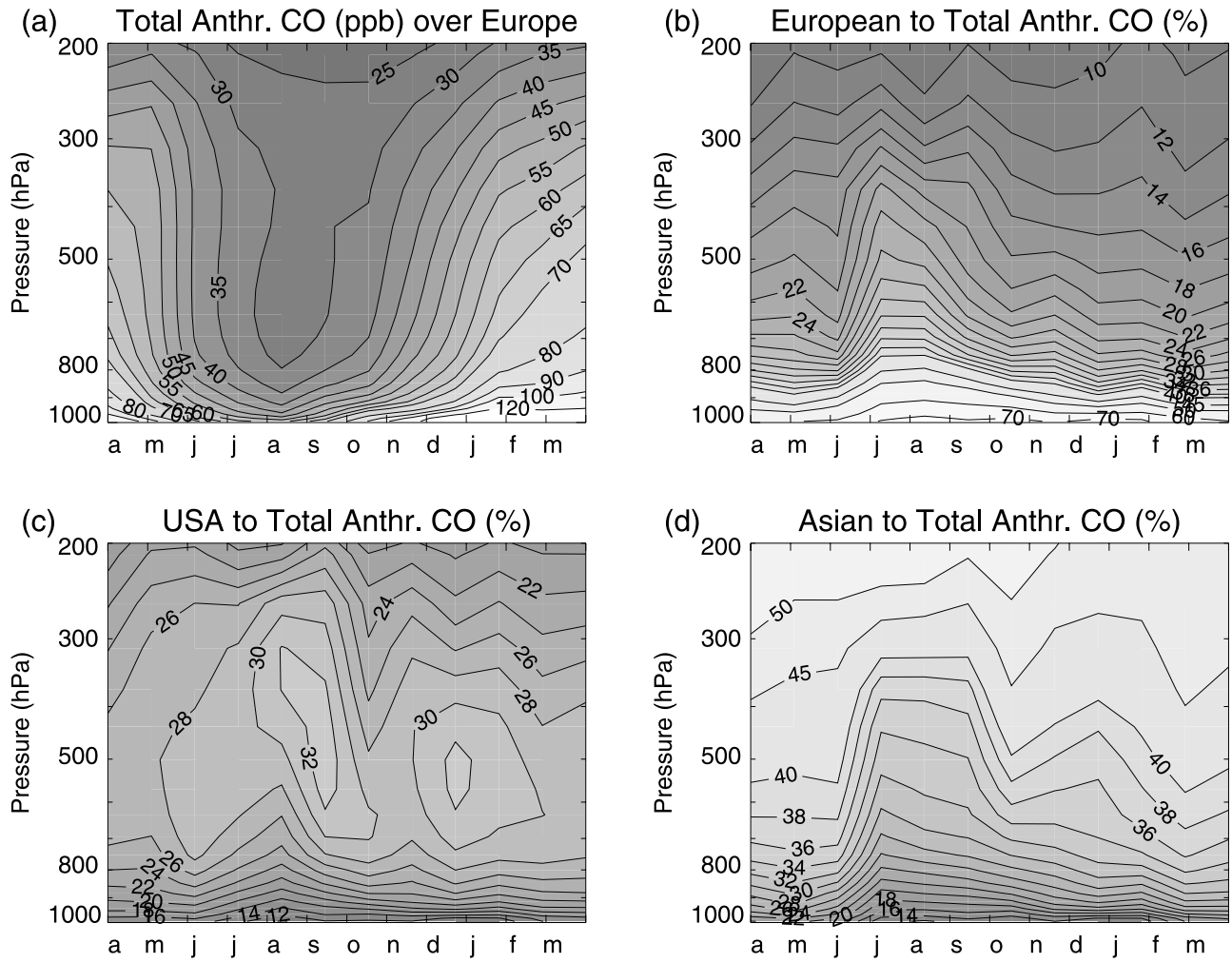

Figure 10. (a) Total anthropogenic CO (ppb) over Europe as a function of time and altitude. (b–d) Contribution (%) of anthropogenic CO emissions from sources in Europe, Asia, and North America to the anthropogenic CO load over Europe as a function of time and altitude.

[52] *Li et al.* [2002] conclude from their studies that one pathway for transatlantic transport of CO and ozone from North America to Europe takes place in the lower troposphere year-round favored by the relatively short distance between the two continents and the fact that the prevailing westerlies extend down to the surface essentially year-round over the eastern USA. Other pathways include transport by warm conveyor belts [*Cooper et al.*, 2002; *Stohl et al.*, 2002; *Eckhardt et al.*, 2004] and strong convection over the eastern and central USA lifting pollutants into the middle and upper troposphere followed by transport by the westerlies. The latter mechanism is especially frequent in summertime.

[53] As shown in section 5.2.1, Asian sources are strong in magnitude, and for most altitudes the impact of Asian sources on the anthropogenic CO burden over Europe is larger than the impact of North American sources (Figure 9). On average, the fraction of anthropogenic CO coming from Asia and averaged over the region Europe is ~3% each at the surface for emitters both in north Asia and in India, and 9% for CO emitted from sources in China. The impact from Southeast Asian pollutants is minor even though the emissions are about 2.5 times stronger than for north Asia. Except for sources from north Asia, the contributions are steadily increasing with increasing altitude in the atmosphere. At 200 hPa the annual mean contributions are 13%, 31%, and 4% for India, China, and Southeast Asia, respectively. CO levels from north Asian sources reach maximum contributions (~5%) at altitudes between about 500–800 hPa. The main contributors from Asia are therefore sources in China and India, i.e., the two regions that also provide large surface CO sources. The largest Asian contributions (Figure 10c) are typically observed around springtime, which actually coincides with the time of the year when the outflow from Asia has been shown to be most effectively directed toward the west [*Newell and Evans*, 2000]. In winter, the effect of the Siberian anticyclone leads to the input of pollutants into the tropical region, while during spring and summer convection allows pollution to more likely escape the boundary layer and enter the middle to upper tropospheric westerlies.

[54] CO sources in Africa north of the equator show less impact on the CO field over Europe compared to Asian and North American emissions and they most strongly affect the southern part of Europe (not shown here). Near the surface, about 2% of the anthropogenic CO concentrations averaged

over Europe originate from sources in North Africa on an annual mean, and the impact increases with increasing altitude to about 6% at 500 hPa and 9% at 200 hPa.

6. Summary and Conclusions

[55] CO concentrations provided by the MOPITT remote sensing instrument, as well as ground-based in situ measurements have been used to evaluate simulations of the CO field over Europe performed with the global chemistry transport model MOZART-2. The model simulations in turn served as a basis for a budget analysis looking into the contributions of various source regions and source types to the CO mixing ratios over Europe.

[56] The model simulations are based on a set of optimized emissions derived from a Bayesian synthesis inversion scheme using CO concentrations derived from MOPITT data and model simulations. The agreement with MOPITT retrieved CO data clearly improved when the optimized emissions were employed in MOZART, and the agreement with independent surface in situ measurements (i.e., data that were not used in the surface emission inversion) showed an improvement at some of the locations. The inversion scheme optimizes the surface emissions of an entire region. The agreement for the entire region is improving, however, for selected locations this might not be true because uncertainties in the spatial distribution of sources within a domain are not corrected for in the optimization. This implies that the selection of the regions used in the inversion scheme needs to be carefully chosen according to the scientific studies planned or vice versa.

[57] The comparison of the observed CO concentrations with the model values indicate that the model is capable of representing background conditions as well as the transport over large scales relatively well, and is therefore well suited for the budget analysis conducted. Largest differences occur close to the surface as the model does not reflect the variability in surface emissions or transport on small scales. This is due to the coarse spatial resolution and various assumptions and simplifications in the model calculations. The intercomparison showed that the model concentrations over Europe tend to be too low in spring and too high in autumn. The latter effect is most pronounced at high latitudes. The monthly mean differences between MOPITT and MOZART CO mixing ratios averaged over Europe, are in the range of about ±20 ppb for low altitude levels, and within about ±10 ppb at higher altitude levels, which is comparable to the uncertainty of the observations.

[58] As CO is a suitable tracer for atmospheric transport we use the model simulations of CO to diagnose processes contributing to the concentrations over Europe for an altitude range from the surface up to about 200 hPa. Results from a "tagged run," i.e., simulations where the CO is tagged according to the type of source and the source region, have been performed for this purpose. We set the focus on the "anthropogenic" CO concentrations defined as CO originating from technological activities, biofuel use, and biomass burning. CO from these sources accounts for about 40–70% of the total CO near the surface over Europe, and for about 30–60% at 500 hPa.

[59] Averaged over the region Europe the largest contribution (67% on an annual mean) to the anthropogenic CO load over Europe at the surface comes from regional sources. Further significant impact is evident from sources in North America (14%) and Asia (15%). With increasing altitude the influence of European sources weakens, and the impact of other source regions, especially Asia and North America gains in importance. Asian emissions seem to be more important than North American emissions during most months and at most heights. The largest contribution for CO from Asian sources is observed at highest altitudes (about 50% at 200 hPa), and at about 500 hPa for CO coming from sources in North America (32%). CO from sources in North Africa contributes by about 2% close to the surface, and ~9% at 200 hPa to the anthropogenic CO mixing ratios over Europe, and strongest impact is evident over southern Europe. The seasonal and altitude dependent patterns seen in the contributions for sources in Europe, Asia, and North America will be subject to future studies.

[60] The results indicate how expected source changes might impact the European CO field, e.g., increased emissions from Asia will have a stronger impact on Europe than changes in African sources. Our studies also reveal how the combination of modeled and observed CO data may improve the usefulness of simulated CO fields by (1) including observations to optimize the model input parameter (i.e., the surface emissions) and (2) evaluating the model simulations by comparison with observations.

[61] Satellite observations like MOPITT are of great use in the evaluation of model simulations because they provide near-global coverage and represent continuous data series over a long time period. However, there are also some essential limitations and, because of the retrieval characteristics, care in the interpretation and application of remote sensing data is required. For example, MOPITT has a low measurement sensitivity near the surface and is not well suited to validate the performance of the boundary layer ventilation in chemistry transport models. It is also important to understand that even though the MOPITT retrieval provides the CO mixing ratio at seven atmospheric levels, these levels are not entirely independent from each other, limiting the significance of the model evaluation with regard to the vertical resolution. Hence the involvement of other types of measurements such as in situ measurements is necessary and helps evaluating the model over a broad range of temporal and spatial coverage and resolution.

[62] The results from the model evaluation indicate that studies considering the temporal and spatial variability on a large scale (i.e., intercontinental transport, monthly averages) are feasible based on the simulations. The intercontinental transport to Europe is only one aspect that may be looked at with the techniques applied in the presented work. The range of applications for this type of study is far-reaching, and may include studies concentrating on the transport to and from other regions as well as the dispersion of CO from different source types.

[63] **Acknowledgments.** Funding for the work for G. Pfister is provided by the Erwin-Schroedinger Fellowship of the Austrian Science Foundation and by the NCAR Visiting Scientist Program. Work of G. Pétron is supported by the EOS Interdisciplinary Science Program (EOS/IDS), the European Commission under the POET project (EVK2-1999-00011), by the Program "Gestion et Impacts du Changement Climatique" of the French Ministry of Environment and by the French National Program for Atmospheric Chemistry (PNCA). The NCAR MOPITT project is supported by the National Aeronautics and Space Administration (NASA) Earth

Observing System (EOS) Program. The National Center for Atmospheric Research (NCAR) is sponsored by the National Science Foundation. The authors would like to thank the Austrian Environmental Agency and the Climate Monitoring and Diagnostics Laboratory for providing ground-based data of CO. We thank Merritt Deeter, Peter Hess, and two anonymous reviewers for helpful comments.

References

Allen, D. J., P. Kasibhatla, A. M. Thompson, R. B. Rood, B. G. Doodridge, K. E. Pickering, R. D. Hudson, and S. J. Lin (1996), Transport-induced interannual variability of carbon monoxide determined using a chemistry and transport model, *J. Geophys. Res.*, *101*, 28,655–29,669.

Bergamaschi, P., R. Hein, M. Heimann, and P. J. Crutzen (2000), Inverse modeling of the global CO cycle: 1. Inversion of CO mixing ratios, *J. Geophys. Res.*, *105*, 1909–1927.

Bey, I., D. J. Jacob, R. M. Yantosca, J. A. Logan, B. D. Field, A. M. Fiore, Q. Li, H. Liu, L. J. Mickley, and M. G. Schultz (2001a), Global modeling of tropospheric chemistry with assimilated meteorology: Model description and evaluation, *J. Geophys. Res.*, *106*, 23,073–23,095.

Bey, I., D. J. Jacob, J. A. Logan, and R. M. Yantosca (2001b), Asian chemical outflow to the Pacific: Origins, pathways, and budgets, *J. Geophys. Res.*, *106*, 23,097–23,113.

Brasseur, G., D. A. Hauglustaine, and S. Walters (1996), Chemical compounds in the remote Pacific troposphere: Comparison between MLOPEX measurements and chemical transport model calculations, *J. Geophys. Res.*, *101*, 14,795–14,813.

Brasseur, G. P., D. A. Hauglustaine, S. Walters, P. J. Rasch, J.-F. Mueller, C. Granier, and X. X. Tie (1998), MOZART: A global chemistry transport model for ozone and related chemical tracers: 1. Model description, *J. Geophys. Res.*, *103*, 28,265–28,290.

Cooper, O. R., J. L. Moody, D. D. Parrish, M. Trainer, J. S. Holloway, G. Hübler, F. C. Fehsenfeld, and A. Stohl (2002), Trace gas composition of midlatitude cyclones over the western North Atlantic Ocean: A seasonal comparison of O_3 and CO, *J. Geophys. Res.*, *107*(D7), 4057, doi:10.1029/2001JD000902.

Deeter, M. N., et al. (2003), Operational carbon monoxide retrieval algorithm and selected results for the MOPITT Instrument, *J. Geophys. Res.*, *108*(D14), 4399, doi:10.1029/2002JD003186.

Drummond, J. R., and G. S. Mand (1996), The Measurements of Pollution in the Troposphere (MOPITT) Instrument: Overall performance and calibration requirements, *J. Atmos. Oceanic Technol.*, *13*, 314–320.

Eckhardt, S., A. Stohl, H. Wernli, P. James, C. Forster, and N. Spichtinger (2004), A 15-year climatology of warm conveyor belts, *J. Clim.*, *17*(1), 218–237.

Emmons, L. K., et al. (2004), Validation of Measurements of Pollution in the Troposphere (MOPITT) CO retrievals with aircraft in situ profiles, *J. Geophys. Res.*, *109*, D03309, doi:10.1029/2003JD004101.

Forster, C., et al. (2001), Transport of boreal forest fire emissions from Canada to Europe, *J. Geophys. Res.*, *106*, 22,887–22,906.

Fraser, P. J., P. Hyson, R. A. Rasmussen, A. J. Crawford, and M. A. K. Khalil (1986), Methane, carbon monoxide, and methylchloroform in the Southern Hemisphere, *J. Atmos. Chem.*, *4*, 3–42.

Graedel, T. E., et al. (1993), A compilation of inventories of emissions to the atmosphere, *Global Biogeochem. Cycles*, *7*(1), 1–26.

Granier, C., G. Petron, J.-F. Mueller, and G. Brasseur (2000), The impact of natural and anthropogenic hydrocarbons on the tropospheric budget of carbon monoxide, *Atmos. Environ.*, *34*, 5255–5270.

Horowitz, L. W., et al. (2003), A global simulation of tropospheric ozone and related tracers: Description and evaluation of MOZART, version 2, *J. Geophys. Res.*, *108*(D24), 4784, doi:10.1029/2002JD002853.

Lamarque, J.-F., and P. G. Hess (2003), Model analysis of the temporal and geographical origin of the CO distribution during the TOPSE campaign, *J. Geophys. Res.*, *108*(D4), 8354, doi:10.1029/2002JD002077.

Levy, H., II, P. S. Kasibhatla, W. J. Moxim, A. A. Klonecki, A. L. Hirsch, S. J. Oltmans, and W. L. Chameides (1997), Global impact of human activity on tropospheric ozone, *Geophys. Res. Lett.*, *24*, 791–794.

Li, Q., et al. (2002), Transatlantic transport of pollution and its effect on surface ozone in Europe and North America, *J. Geophys. Res.*, *107*(D13), 4166, doi:10.1029/2001JD001422.

Müller, J. F. (1992), Geographical distribution and seasonal variation of surface emissions and deposition velocities of atmospheric trace gases, *J. Geophys. Res.*, *97*, 3787–3804.

Newell, R. E., and M. J. Evans (2000), Seasonal changes in pollutant transport to the North Pacific: The relative importance of Asian and European sources, *Geophys. Res. Lett.*, *27*, 2509–2512.

Novelli, P. C., L. P. Steele, and P. P. Tans (1992), Mixing ratios of carbon monoxide in the troposphere, *J. Geophys. Res.*, *97*, 20,731–20,750.

Novelli, P. C., J. E. Collins Jr., R. C. Myers, G. W. Sachse, and H. E. Scheel (1994), Reevaluation of the NOAA/CMDL carbon monoxide reference scale and comparison with CO reference gases at NASA-Langley and the Fraunhofer Institut, *J. Geophys. Res.*, *99*, 12,833–12,839.

Novelli, P. C., K. A. Masarie, and P. M. Lang (1998), Distributions and recent changes of carbon monoxide in the lower troposphere, *J. Geophys. Res.*, *103*, 19,015–19,033.

Novelli, P. C., K. A. Masarie, P. M. Lang, B. D. Hall, R. C. Myers, and J. W. Elkins (2003), Details for reanalysis of tropospheric CO trends: Effects of the 1997–1998 wildfires, *J. Geophys. Res.*, *108*(D15), 4464, doi:10.1029/2002JD003031.

Olivier, J., J. Peters, C. Granier, G. Pétron, J. F. Müller, and S. Wallens (2003), Present and future surface emissions of atmospheric compounds, *POET rep. 2, EU proj. EVK2-1999-0001111*, Eur. Union, Brussels.

Pétron, G. (2003), Modélisation inverse des émissions du monoxyde de carbone, Ph.D. thesis, Univ. de Paris 6, Paris.

Pinto, J. P., Y. L. Yung, D. Rind, G. L. Russel, J. A. Lerner, J. E. Hansen, and S. Hameed (1983), A general circulation model study of atmospheric carbon monoxide, *J. Geophys. Res.*, *88*, 3691–3702.

Reichle, H., Jr., et al. (1999), Space shuttle based global CO measurements during April and October 1994, MAPS instrument, data reduction, and data validation, *J. Geophys. Res.*, *104*, 21,443–21,454.

Rodgers, C. D. (2000), *Inverse Methods for Atmospheric Sounding, Theory and Practice*, World Sci., River Edge, N. J.

Seiler, W. (1974), The cycle of atmospheric CO, *Tellus*, *Ser. B*, *26*, 118–135.

Stohl, A., and T. Trickl (1999), A textbook example of long-range transport: Simultaneous observation of ozone maxima of stratospheric and North American origin in the free troposphere over Europe, *J. Geophys. Res.*, *104*, 30,445–30,462.

Stohl, A., S. Eckhardt, C. Forster, P. James, and N. Spichtinger (2002), On the pathways and timescales of intercontinental air pollution transport, *J. Geophys. Res.*, *107*(D23), 4684, doi:10.1029/2001JD001396.

Stohl, A., C. Forster, S. Eckhardt, N. Spichtinger, H. Huntrieser, J. Heland, H. Schlager, S. Wilhelm, F. Arnold, and O. Cooper (2003), A backward modeling study of intercontinental pollution transport using aircraft measurements, *J. Geophys. Res.*, *108*(D12), 4370, doi:10.1029/2002JD002862.

Warneck, P. (2000), *Chemistry of the Natural Atmosphere*, 927 pp., Academic, San Diego, Calif.

Warner, J. X., J. C. Gille, D. P. Edwards, D. C. Ziskin, M. W. Smith, P. L. Bailey, and L. Rokke (2001), Cloud detection and clearing for the Earth Observing System Terra satellite Measurements of Pollution in the Troposphere (MOPITT) experiment, *Appl. Opt.*, *40*, 1269–1284.

Wild, O., and H. Akimoto (2001), Intercontinental transport of ozone and its precursors in a three-dimensional global CTM, *J. Geophys. Res.*, *106*, 27,729–27,744.

J.-L. Attie, Laboratoire d'Aerologie, Observatoire Midi Pyrénées, 14 Avenue Edouard Belin, F-31400 Toulouse, France.

C. Granier, Service d'Aéronomie, Université Paris 6, 4 Place Jussieu, F-75252 Paris Cedex 05, France.

D. P. Edwards, L. K. Emmons, J. C. Gille, J.-F. Lamarque, and G. Pfister, Atmospheric Chemistry Division, National Center for Atmospheric Research, P. O. Box 3000, Boulder, CO 80307, USA. (pfister@ucar.edu)

P. C. Novelli, NOAA Climate Monitoring and Diagnostics Laboratory, 325 Broadway, Boulder, CO 80305, USA.

G. Pétron, Advanced Study Program, National Center for Atmospheric Research, Box 3000, Boulder, CO 80307, USA.